The Paris Agreement objectives will likely halt future declines of emperor penguins

Stéphanie Jenouvrier, Marika Holland, David Iles, Sara Labrousse, Laura Landrum, Jimmy Garnier, Hal Caswell, Henri Weimerskirch, Michelle Larue, Rubao Ji, et al.

The Paris Agreement objectives will likely halt future declines of emperor penguins

Stéphanie Jenouvrier, Marika Holland, David Iles, Sara Labrousse, Laura Landrum, Jimmy Garnier, Hal Caswell, Henri Weimerskirch, Michelle Larue, Rubao Ji, et al.

The Paris Agreement objectives will likely halt future declines of emperor penguins

Stéphanie Jenouvrier[1,2] | Marika Holland[3] | David Iles[1] | Sara Labrousse[1] | Laura Landrum[3] | Jimmy Garnier[4] | Hal Caswell[1,5,6] | Henri Weimerskirch[2] | Michelle LaRue[7,8] | Rubao Ji[1] | Christophe Barbraud[2]

[1]Biology Department, Woods Hole Oceanographic Institution, Woods Hole, MA, USA

[2]Centre d'Etudes Biologiques de Chizé, UMR 7372 du Centre National de la Recherche Scientifique-Université de La Rochelle, Villiers en Bois, France

[3]National Center for Atmospheric Research, Boulder, CO, USA

[4]Laboratoire de Mathématiques, UMR 5127, Université Savoie Mont-Blanc, Le Bourget du Lac, France

[5]Max Planck Institute for Demographic Research, Rostock, Germany

[6]University of Amsterdam, Amsterdam, The Netherlands

[7]Te Kura Aronukurangi, University of Canterbury, Christchurch, New Zealand

[8]Department of Earth and Environmental Sciences, University of Minnesota, Minneapolis, MN, USA

Correspondence
Stéphanie Jenouvrier, Biology Department, MS-34, Woods Hole Oceanographic Institution, Woods Hole, MA, USA.
Email: sjenouvrier@whoi.edu

Funding information
NSF, Grant/Award Number: 1643901 and 1744794

Abstract

The Paris Agreement is a multinational initiative to combat climate change by keeping a global temperature increase in this century to 2°C above preindustrial levels while pursuing efforts to limit the increase to 1.5°C. Until recently, ensembles of coupled climate simulations producing temporal dynamics of climate en route to stable global mean temperature at 1.5 and 2°C above preindustrial levels were not available. Hence, the few studies that have assessed the ecological impact of the Paris Agreement used ad-hoc approaches. The development of new specific mitigation climate simulations now provides an unprecedented opportunity to inform ecological impact assessments. Here we project the dynamics of all known emperor penguin (*Aptenodytes forsteri*) colonies under new climate change scenarios meeting the Paris Agreement objectives using a climate-dependent-metapopulation model. Our model includes various dispersal behaviors so that penguins could modulate climate effects through movement and habitat selection. Under business-as-usual greenhouse gas emissions, we show that 80% of the colonies are projected to be quasiextinct by 2100, thus the total abundance of emperor penguins is projected to decline by at least 81% relative to its initial size, regardless of dispersal abilities. In contrast, if the Paris Agreement objectives are met, viable emperor penguin refuges will exist in Antarctica, and only 19% and 31% colonies are projected to be quasiextinct by 2100 under the Paris 1.5 and 2 climate scenarios respectively. As a result, the global population is projected to decline by at least by 31% under Paris 1.5 and 44% under Paris 2. However, population growth rates stabilize in 2060 such that the global population will be only declining at 0.07% under Paris 1.5 and 0.34% under Paris 2, thereby halting the global population decline. Hence, global climate policy has a larger capacity to safeguard the future of emperor penguins than their intrinsic dispersal abilities.

KEYWORDS
Antarctica, climate change mitigation, dispersion, emission reduction pledges, seabirds

1 | INTRODUCTION

The Paris Agreement is a multinational initiative to curb future atmospheric warming, with an explicit goal of limiting the global temperature increase to 'well below 2°C', and ideally to 1.5°C relative to the preindustrial mean (UNFCCC, 2015). Pathways to reach the Paris Agreement objectives require globally unified climate policy in the short-term, and transformation of global energy supply, including large-scale shifts away from fossil fuel use and increasing investment in renewable energies, combined with carbon dioxide removal through afforestation (Rogelj et al., 2018). The Paris Agreement therefore represents global recognition of the importance of pursuing climate change solutions in the near-term.

Global-scale vulnerability assessments based on species traits and expert opinion indicate that over one-quarter of birds, amphibians, and corals are highly vulnerable to 2°C degrees of warming (Foden et al., 2013). Recently, Warren, Price, Graham, Forstenhaeusler, and VanDerWal (2018) reported widespread projected range loss in insects, plants, and vertebrates under current emissions pledges, but meeting the Paris Agreement 1.5°C objective would dramatically curb these range contractions. However, projected range contractions do not necessarily correspond directly to changes in population abundance (Ehrlén & Morris, 2015; Schurr et al., 2012). Instead, mechanistic models that link climate to demographic processes are required to account for the complex population responses that can arise under scenarios of future change (Jenouvrier, 2013). Unfortunately, climate-coupled demographic projections are rare because they require detailed, long-term, longitudinal data. Indeed, only 18 studies have used this approach to project the future abundance of bird populations under specific climate change scenarios (reviewed in Iles & Jenouvrier, 2019). No studies have yet explicitly examined the consequences of meeting the Paris Agreement objectives on population dynamics for any species.

Climate change occurs differently among regions (Stocker et al., 2013), resulting in a shifting mosaic of habitat quality across a species' range (McRae et al., 2008; Travis et al., 2013). On ecological timescales, population viability of sensitive species will therefore depend on the capacity for individuals to disperse to suitable habitats. Yet, dispersal generates complex population-level responses to environmental change, including 'ecological traps' or 'attractive sinks' (Kristan, 2003), rescue effects, emergent metapopulation synchrony (Lande, Engen, & Sæther, 1999), and habitat-structured transient dynamics (Iles, Williams, & Crone, 2018). These effects can either dampen or amplify species' sensitivity to climate change (Bowler & Benton, 2005; Travis et al., 2013). Predicting population responses to climate change therefore requires a full consideration of species' dispersal capabilities (Travis et al., 2012). However, most quantitative projections of species abundance under future climate ignore this important mechanism (Travis et al., 2013) and the relative extent to which dispersal and global climate policy can reduce the projected species extinction of climate change is an open question (Warren, Price, VanDerWal, Cornelius, & Sohl, 2018).

Finally, accurately assessing future climate impacts on ecosystems requires the use of fully coupled climate models that track the nonlinear temporal evolution of the ocean–atmosphere system (Jenouvrier, 2013). Until recently, ensembles of internally consistent coupled climate simulations that produce stable equilibrium global mean temperature at 1.5 and 2°C above preindustrial levels were not available. The development of these specific mitigation models (Sanderson et al., 2017) now provides an unprecedented opportunity to examine the temporal climate dynamics that would result from meeting the Paris Agreement objectives, and their concomitant effects on natural populations. Correctly representing the temporal evolution of climate under the Paris Agreement is particularly important for understanding wildlife responses because short-term rates of population change and historical 'legacy' effects can strongly influence population viability (Lande, 1993). To date, no studies have used these mitigation climate models to inform ecological impact assessments.

Emperor penguins (*Aptenodytes forsteri*) are iconic examples of a species threatened by future climate change (Barbraud & Weimerskirch, 2001; Forcada & Trathan, 2009; Jenouvrier, Caswell, et al., 2009; Jenouvrier, Garnier, Patout, & Desvillettes, 2017; Jenouvrier et al., 2014; Ropert-Coudert et al., 2019). The emperor penguin is classified as 'near threatened' by the International Union for the Conservation of Nature and is currently under consideration for inclusion under the United States Endangered Species Act. Beyond these focused conservation measures, can near-term global action on climate policy curb the projected declines of emperor penguin populations?

Projections indicate that most breeding colonies will be endangered by 2100 under 'business as usual' emissions scenarios (Jenouvrier et al., 2014), resulting in dramatic declines in the global population size even under optimistic dispersal scenarios (Jenouvrier et al., 2017). These declines occur through projected loss of Antarctic sea ice, to which the emperor penguin life cycle is closely tied. Emperor penguins directly rely on seasonally stable sea ice as a breeding platform during the Antarctic winter and throughout the spring chick-rearing period (Ainley et al., 2010). During the nonbreeding season, sea ice serves as a platform from which they feed, molt, and seek refuge from predators. Sea ice also influences critical components of the food chain (e.g., krill: *Euphausia superba* and silverfish: *Pleuragramma Antarctica*; La Mesa et al., 2010; Meyer et al., 2017). Therefore, sea ice conditions affect the survival and reproduction of emperor penguins both directly (e.g., early sea ice breakup can jeopardize chick survival) and indirectly through the food web (Abadi, Barbraud, & Gimenez, 2017; Jenouvrier, Barbraud, Weimerskirch, & Caswell, 2009; Jenouvrier et al., 2012). Specifically, the breeding success is reduced in years with higher sea ice cover because foraging trips are longer, energetic costs for adults are higher, and offspring provisioning is lower (Jenouvrier et al., 2012; Massom et al., 2009; Zimmer et al., 2008). In addition, adult survival is maximized at intermediate levels of sea ice because neither the complete absence of sea ice (low food resources and/or high predation),

nor heavy and persistent sea ice (longer foraging trip), provide satisfactory conditions (Jenouvrier et al., 2012).

Here we provide a global assessment of the potential impacts of limiting global warming to 1.5 or 2°C on emperor penguins using a set of new climate scenarios, and compare the importance of biological mechanisms for a species to cope with climate change (i.e., dispersal) with the ability of meeting the Paris Agreements. We utilize a unique ensemble of transient climate simulations which are subject to emissions scenarios that have been specifically designed to meet the Paris Agreement targets (Sanderson et al., 2017) and provide the first analysis of Antarctic sea ice conditions in these simulations. Our study integrates these new climate projections with a mechanistic metapopulation model previously developed by Jenouvrier, Caswell, Barbraud, and Weimerskirch (2010) and Jenouvrier et al. (2012, 2014, 2017), providing fundamental insight into the capacity for near-term global action on climate policy to alter the future of an iconic marine predator.

2 | MATERIALS AND METHODS

Our analysis focuses on estimating the demographic responses of emperor penguin populations to three climate scenarios, each representing a distinct future that is contingent on human policy decisions in the near-term. There are 54 known emperor penguin colonies around the coast of Antarctica (Fretwell et al., 2012; Fretwell & Trathan, 2009; LaRue, Kooyman, Lynch, & Fretwell, 2015; Figure S1). Emperor penguins breed in large colonies (>100 individuals) on sea ice, forming a set of discrete, yet potentially connected local populations over the entire species range along the Antarctic coast. Hence, we link the new simulations of future sea ice conditions to a metapopulation model developed by Jenouvrier et al. (2010, 2012, 2014, 2017). The metapopulation model describes the demography and dispersal behavior of emperor penguins across their Antarctic range. It includes vital rates (survival and reproduction) that depend on the mean sea ice conditions during four seasons of the emperor penguin life cycle (nonbreeding, laying, incubating, and rearing), and accounts for differences in the impact of sea ice conditions on adult survival between males and females. In the sections below, we more fully describe climate scenario and sea ice projections, as well as dispersal scenario and the sea ice-dependent metapopulation model. In addition, in order to assess the consequence of potential biases in sea ice simulations, we performed a sensitivity analysis of the sea ice-dependent metapopulation model to quantify which of the sea ice seasonal means affect the most the population growth rate projected at each colony throughout this century. Finally, we analyze the uncertainties of the sea ice-dependent metapopulation model.

2.1 | Climate scenarios

Our new analysis incorporates two unique mitigation scenarios developed by the National Center for Atmospheric Research using a General Circulation Model (GCM) to explicitly evaluate future climate trajectories under the Paris Agreement temperature targets (described in Sanderson et al., 2017). These mitigation scenarios are unique in that they were explicitly designed to meet the global temperature change targets set in the Paris Agreement (Sanderson & Knutti, 2016). This is in contrast to other emissions scenarios, for example, the SRES (Special Report on Emissions Scenarios; Nakicenovic et al., 2000) or the representative concentration pathways (RCP; Van Vuuren et al., 2011) scenarios used in the fourth and fifth IPCC assessment reports, respectively. While these older scenarios consider a range of possible human activity and resulting greenhouse gas emissions, they had no explicit consideration of the Paris Agreement targets and hence do not lead to a 1.5 or 2°C global average warming by 2100. Previous ecological studies have instead used ad hoc approaches to obtain climate projections meeting the Paris Agreement temperature targets using RCP scenario simulations (e.g., Warren, Price, Graham, et al., 2018).

Furthermore, we compare the resulting emperor penguin population projections obtained with these two new Paris scenario to those obtained from a 'business-as-usual' climate scenario (RCP 8.5; Meinshausen et al., 2011) that represents a future in which greenhouse gas emissions continue unabated. By using climate simulations with these new Paris Agreement scenarios, we are able to directly consider the avoided impacts for emperor penguins in 1.5 or 2°C climate futures relative to a 'business-as-usual' scenario. The RCP 8.5 scenario uses the same Community Earth System Model (CESM) model and includes a large ensemble of simulations (Kay et al., 2015), allowing us to assess the importance of internal variability. This model was contributed to the Coupled Model Intercomparison Project 5 (CMIP5) and included in the IPCC fifth assessment report. Previous studies have projected emperor penguin populations under 'business-as-usual' climate scenarios (SRES A1.B) using the climate model ensemble from the IPCC's fourth assessment report, that is, CMIP3 multimodel dataset (Jenouvrier et al., 2012, 2014). The CMIP3 includes older generation models than that available in CMIP5 and a direct comparison between the climate projections from CMIP3 and CMIP5 is not possible because they use different scenarios describing the amount of greenhouse gas in the atmosphere in the future (SRESs: Nakicenovic et al., 2000 vs. RCPs: Van Vuuren et al., 2011, respectively). However, for both large-scale climate patterns and the magnitudes of climate change, there is overall consistency between the projections based on CMIP3 and CMIP5 (Stocker et al., 2013).

2.2 | Sea ice projections

The climate model simulations used in this study are produced from the CESM using the Community Atmosphere Model, version 5 (CESM1-CAM5; Hurrell et al., 2013). This is a fully coupled earth system model which incorporates atmosphere, ocean, sea ice and terrestrial components. It has a nominal 1° resolution in both the atmosphere and the ocean. This model has a very good overall simulation of climate as compared to other models (e.g., Knutti & Sedláček, 2013) and numerous aspects of the Antarctic climate, such as wind

variability and the sea ice response to that variability (e.g., Landrum, Holland, Raphael, & Polvani, 2017), are well simulated. Our use of a large ensemble of simulations allows us to quantify the uncertainties related to internal climate variability.

Specifically, we use simulations from the CESM Large Ensemble project (CESM-LENS; Kay et al., 2015) which include 40 ensemble members run from 1920–2100 with historical forcings over the 20th century and the RCP 8.5 21st-century emissions scenario. These are compared to Paris target agreement simulations (Sanderson et al., 2017) which employ emissions scenarios that result in a 1.5°C global average warming (Paris 1.5) or a 2°C global average warming (Paris 2) by 2100. All simulations use the identical climate model and the Paris target simulations are branched from the CESM-LENS simulations in 2006 and run from 2006–2100. We calculate the seasonal sea ice conditions means for the four seasons of the life cycle of the emperor penguin, at each colony, following the approach described by Jenouvrier et al. (2014). Here we present for the first time, the projection of sea ice in Antarctica from these unique climate ensembles.

2.3 | Dispersal scenarios

Individual dispersal behaviors for emperor penguins are poorly understood because emperor penguin have been marked at only one site (Pointe Géologie; Wienecke, 2011), and no recapture occurred at other colonies. Until recently, emperor penguins were considered to be highly philopatric (Prevost, 1961). Recent studies have now shown some degree of genetic homogenization for emperor penguin colonies, suggesting high connectivity in these populations via individual dispersal among colonies (Clucas et al., 2018; Younger et al., 2017). In addition, recent work suggests that emperor penguin colonies can move onto ice shelves and perhaps found new colonies (Fretwell et al., 2012; Fretwell, Trathan, Wienecke, & Kooyman, 2014).

Hence, we explore various scenarios combining different dispersal rates, dispersal behaviors, and dispersal distances (see Jenouvrier et al., 2017 for more details). Our sea ice-dependent metapopulation model assumes that individuals only emigrate from poor quality breeding sites when environmental conditions lead to negative fitness. With an informed search, individuals select habitats that maximize fitness within their dispersal range; this behavior occurs among some colonial seabirds that prospect for breeding sites using the presence and reproductive success of residents (Doligez, Danchin, & Clobert, 2002). In contrast, random search behavior results in undirected movements with respect to habitat quality. The short-distance dispersal scenario allows for regional movements among colonies, while long-distance dispersal creates a more connected metapopulation across the entire continent.

2.4 | Sea ice-dependent metapopulation model

The sea ice-dependent metapopulation model was developed by Jenouvrier et al. (2017) using MATLAB R2018, The MathWorks, Inc., Natick, Massachusetts, United States. The model projects the population vector $\mathbf{n}$—comprising the population size n_i in each colony i—from time t to $t + 1$ using:

$$\mathbf{n}(t+1) = \mathbf{D}[\mathbf{x}(t), \mathbf{n}(t)]\mathbf{F}[\mathbf{x}(t), \mathbf{n}(t)]\mathbf{n}(t), \quad (1)$$

to indicate that the projection interval is divided into two main phases of possibly different duration: the reproduction phase ($\mathbf{F}$) followed by the dispersal phase ($\mathbf{D}$).[1] The reproduction matrix $\mathbf{F}$ is constructed using the density-dependent Ricker model. The dispersal phase ($\mathbf{D}$) combines various dispersal behaviors and dispersal events. The projection matrices $\mathbf{D}$ and $\mathbf{F}$ depend on both the current population density $\mathbf{n}(t)$ and the habitat characteristics (including sea ice concentrations anomalies), $\mathbf{x}(t)$, that vary among colonies and over time, t. The global population size at time t is given by $N_t = \sum_i n_i(t)$.

2.4.1 | Reproduction phase

The reproduction matrix, $\mathbf{F}$, is constructed using the Ricker model including the intrinsic growth rate of each colony $r_i(t)$ and the carrying capacity of each colony K_i. Negative density-dependence effects occur within crowded favorable habitats ($r_i > 0$ and $n_i > K_i$) while populations tend to go extinct within poor habitat colonies ($r_i \leq 0$).

The intrinsic growth rate

For each projection interval t, the intrinsic growth rate of each colony $r_i(t)$ is projected by a nonlinear, stochastic, sea ice-dependent, two-sex, stage-classified matrix $\mathbf{A}[\mathbf{x}(t), \mathbf{n}(t)]$. It is described in more detail in Jenouvrier et al. (2010, 2012). $\mathbf{A}[\mathbf{x}(t), \mathbf{n}(t)]$ includes a sequence of seasonal behaviors (arrival to the colony, mating, breeding) and accounts for differences in adult survival between males and females as function of sea ice concentration anomalies $\mathbf{x}(t)$. $\mathbf{A}[\mathbf{x}(t), \mathbf{n}(t)]$ depends on $\mathbf{n}(t)$ because the reproduction is function of the proportion of males and females within the population through mating processes (Jenouvrier et al., 2010).

The matrix $\mathbf{A}[\mathbf{x}(t), \mathbf{n}(t)]$ includes five stages: male and female prebreeders (birds that have yet to breed for the first time), breeding pairs, and male and female nonbreeders (birds that have bred before but do not do so in the current year). The vital rates describing the transitions between these stages from year t to $t + 1$ includes the probability that an individual of a given stage returns to the breeding site, the probability of mating as a function of the availability of potential mates, the probability of breeding success (raising an offspring given that the female lays an egg), the primary sex ratio (fixed at 0.5), the survival of offspring during the first year at sea, and the annual survival of prebreeders, nonbreeders and male and female breeders.

These vital rates are functions of sea ice concentration anomalies relative to the average from 1979 to 2007 during four seasons: (a) the nonbreeding season from January to March; (b)

[1] In this paper, matrices are denoted by upper case bold symbols (e.g., $\mathbf{F}$) and vectors by lower case bold symbols ($\mathbf{n}$); f_{ij} is the (i, j) entry of the matrix $\mathbf{F}$, n_i is the ith entry of the vector $\mathbf{n}$.

the arrival, copulation, and laying period (April–May), hereafter called the laying period; (c) the incubation period (June–July); (d) the rearing period (August–December). These relationships and their estimations are described in detail in Jenouvrier et al. (2012).

Jenouvrier et al. (2017) estimated the carrying capacity of each colony as $K_i = 2N_0$, with N_0 the initial size of the population observed in 2009 (Fretwell & Trathan, 2009; Jenouvrier et al., 2014).

2.4.2 | The dispersal phase

The model includes intercolony movements. A dispersal event includes the three stages: (a) emigration from the resident colony; (b) search for new colony among other colonies with an average dispersal distance d (transfer); and (c) settlement in a new colony. The duration of the transfer phase can vary, as the final settlement in a new colony may occur after several events (e.g., an individual may not settle in its first choice habitat if that habitat has reached its carrying capacity $n_i \geq K_i$).

In our model, movements of individuals among colonies are divided into two successive dispersal events to account for a time-limited search. Indeed for emperor penguins the breeding season lasts 9 months, and thus the timing for prospecting other colonies during the nonbreeding season is limited. During the first dispersal event ($\mathbf{D}^1$) individuals may select the habitat with highest quality (informed search) or settle in a random habitat. During the second dispersal event ($\mathbf{D}^2$) individuals that reached a saturated colony leave and settle randomly in a new colony (see figure 1 in Jenouvrier et al., 2017). The latter is a way to account for a dispersal cost of gathering information for the informed search (see discussion in Jenouvrier et al., 2017).

The dispersal projection matrix $\mathbf{D}$ is thus

$$\mathbf{D} := \mathbf{D}^2\mathbf{D}^1, \tag{2}$$

and each dispersal matrix $\mathbf{D}^e$ is written

$$\mathbf{D}^e := \mathbf{S}^e[\mathbf{x}]\mathbf{M}^e[\mathbf{x}, \mathbf{n}_e], \tag{3}$$

to indicate that matrices for searching behavior, $\mathbf{S}^e$, and emigration, $\mathbf{M}^e$, depend on the population size at the start of the event (n_e) as well as the environmental conditions $\mathbf{x}(t)$.

The first dispersal event

The emigration rate for each colony i depends on the overall quality of the habitat, which is measured by the median of the realized population growth $\overline{r_i^*}$. The emigration rate increases linearly from $m^1 = 0$ at $\bar{r} \geq 0$ to $m^1 = 1$ at critical value $\overline{r_c^*} < 0$. The emigration matrix thus only depends on the ratio $\overline{\mathbf{r}^*(t)}/\overline{r_c^*}$,

$$\mathbf{M}^1 := \mathbf{M}^1\left[\frac{\overline{\mathbf{r}^*(t)}}{\overline{r_c^*}}\right]. \tag{4}$$

A critical threshold $\overline{r_c^*}$ close to 0, corresponds to high dispersion scenario while a larger negative threshold reflects low dispersion.

Once individuals have left their colonies, we assume that they search for a new colony using two different behaviors: an informed searching behavior ($\mathbf{S}_I$) and a random searching behavior ($\mathbf{S}_R$).

The random search assumes that dispersers randomly seek a colony within the limits of the maximum dispersal distance. Thus the probability of selecting a colony depends on the mean dispersal distance of the emperor penguin, d, and the matrix of distance between colonies (dist(i, j)) included in the vector of habitat descriptors $\mathbf{x}$.

$$\mathbf{S}_R := \mathbf{S}_R[\mathbf{x}, d]. \tag{5}$$

The matrix dist(i, j) corresponds to the coastal distance between colonies i and j derived from the location of know emperor penguin colonies.

Conversely, *the informed search* assumes that dispersers search for the most favorable habitat they can reach; we use $\overline{\mathbf{r}^*}$ as a descriptor of the quality of the habitat. Thus the informed search matrix is also a function of $\overline{r^*}$:

$$\mathbf{S}_I := \mathbf{S}_I[\overline{\mathbf{r}^*(t)}, \mathbf{x}, d]. \tag{6}$$

If the selected colony is not at carrying capacity, individuals settle in this new habitat. However, individuals are not able to settle in colonies that have reached their carrying capacities after the first dispersal event, and will conduct a novel search during the second dispersal event.

The second dispersal event

The surplus individuals leave and randomly settle in another colony regardless of their dispersal strategy in their first event. Thus the emigration matrices depend on the carrying capacity $\mathbf{K}$, the population vector $\mathbf{n}$ at the end of the first dispersal event, and a random search matrix:

$$\mathbf{M}^2 := \mathbf{M}^2[\mathbf{K}, \mathbf{n}] \text{ and } \mathbf{S}^2 := \mathbf{S}_R. \tag{7}$$

2.5 | Sensitivity analysis

We conduct a sensitivity analysis to quantify in which seasons, sea ice conditions (SIC) affect the most the intrinsic population growth rate projected at each colony. Using simulations, we calculate the sensitivity of the population growth rate to a perturbation in SIC over a specific season for each colony, at each time step t from 2009 to 2100, for each demographic projection (including uncertainties in demographic processes). We used a local sensitivity approach by adding a small perturbation (p = 1e − 5) to the large ensemble mean of RCP 8.5 at each specific year, ran the demographic model without dispersion with the perturbed SIC, extracted the population growth rate at each colony, and compared it to the population growth rate without perturbation. We summarized results by showing the absolute value of these sensitivities across demographic simulations and time, as our main question is how robust our demographic model is to potential biases in seasonal SIC projections. We used the large ensemble mean of RCP 8.5 because it shows a larger range of sea ice changes throughout the century, but results are consistent across climate scenarios. More details are shown in Figure S2.

2.6 | Uncertainties

The model includes multiple sources of stochasticity and uncertainties related to climate and demography (Jenouvrier et al., 2012). Climate uncertainty reflects the chaotic temporal evolution of the coupled ocean–atmosphere system (often called 'internal variability'). We used multiple ensemble runs of the same climate model and climate scenario, each with vanishingly small differences in initial climate conditions to account for such uncertainty (Hawkins & Sutton, 2009). Parameter uncertainty describes statistical uncertainty in the estimates of demographic parameters (e.g., survival and reproduction, and their responses to sea ice concentration anomalies, see Jenouvrier et al., 2012). Process variance (i.e., environmental stochasticity) reflects true 'unexplained' temporal variance in demographic rates that is not accounted for by sea ice.

To decompose these various sources of uncertainties in our global projections of population growth rate and size, we used a stepwise, nested approach to estimate sources of uncertainty in projections of future population growth rates (Gauthier, Péron, Lebreton, Grenier, & van Oudenhove, 2016). In step 1, we only include parameter uncertainty in projections. This entails generating repeated demographic projections, where random draws from the sampling distributions for each demographic rate are used to parameterize the metapopulation model. In this step, only a single climate run is used, and unexplained temporal process variance in demographic rates is ignored.

In step 2, for each of the repeated projections in step 1, we conduct an additional series of projections using the range of available climate model ensemble members. Uncertainty in future climate causes projections of sea ice from each ensemble member to diverge, relative to their nearly identical initial conditions. Population projections at this stage thus include uncertainty in climate (estimated from multiple climate model ensemble members), and for each ensemble member, parameter uncertainty arising from a series of demographic projections based on random draws from sampling distributions.

In step 3, for each year of each projection, we randomly draw demographic parameters from distributions describing residual process variance. This incorporates additional unexplained temporal variance in demographic rates that is driven by environmental factors other than sea ice (e.g., variation in predator and prey populations).

3 | RESULTS

3.1 | Comparison of Antarctic sea ice projections to observations

Figure 1 compares Antarctic sea ice conditions simulated by the GCM CESM model to satellite observations for the specific seasons of the emperor penguin life cycle across the entire Antarctic coast. The range of Antarctic sea ice conditions simulated by the climate model overlaps very well with the range of observations over the historical period, except in few regions and seasons. Specifically, the model retains too much sea ice in the Eastern Weddell sea during the nonbreeding period (colonies 1–14) and in the west Pacific Ocean during the rearing period (colonies 30–35).

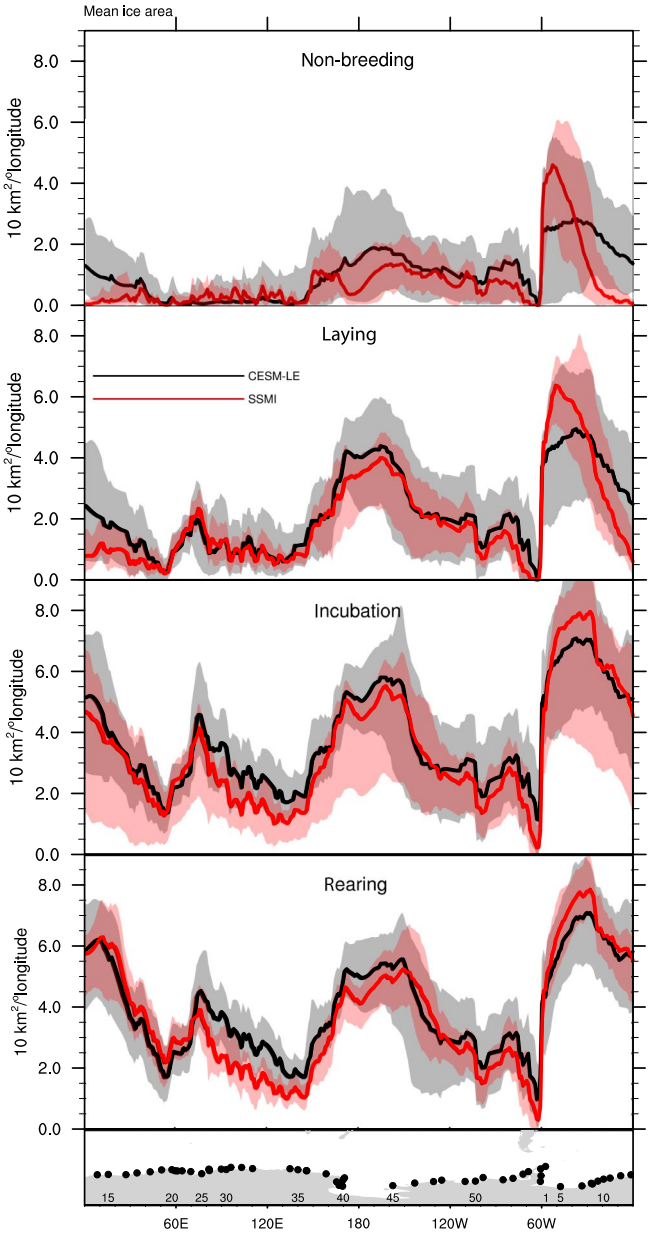

FIGURE 1 Antarctic sea ice extent along the coast of Antarctica from the Community Earth System Model (CESM) and observation for the various seasons of the emperor penguin life cycle (panels). The lower panel shows the Antarctic coast and dots are the location of colonies (Figure S1; Table S1). Inside numbers refer to the emperor colonies, while *x*-labels show longitudes. On the top four panels across seasons, the shading areas show the entire range of Antarctic sea ice extent. In the observations this represents all possible time values 1979–2005 at each longitude for specific season (panel). For the Large Ensemble (CESM-LE), the range represents several runs and all possible time values 1979–2005. The black line is the mean of Antarctic sea ice extent from the large ensemble of CESM, while the red line is the mean of the observations. Sea ice extent is defined as the total area covered by ice of greater than 15% concentration

Our sensitivity analysis reveals that population growth rates are largely influenced by the Antarctic sea ice conditions during the laying season, that are very well resolved in CESM model (Figures 1 and 2). While there are biases in the climatology in the Eastern Weddell during the nonbreeding period, the sensitivity of the population growth rate to sea ice conditions during the nonbreeding is small (Figure 2). While the sensitivity of the growth rate to sea ice conditions during the rearing season is overall relatively large, it varies considerably among colony and time (Figure 2b; Figure S2). These sensitivities are very small for colonies 30–35, locations where the largest differences between the climatology simulated by CESM and observations are observed in the west Pacific Ocean.

3.2 | Antarctic sea ice projections

The largest decline in sea ice conditions relative to historical levels are projected during the nonbreeding and laying seasons of the emperor penguin life cycle, regardless of the climate scenario (Figures 3–5). Large sea ice declines are projected under the 'business-as-usual' climate scenario RCP 8.5, and some colonies are likely to experience complete loss of sea ice during the nonbreeding, incubation,

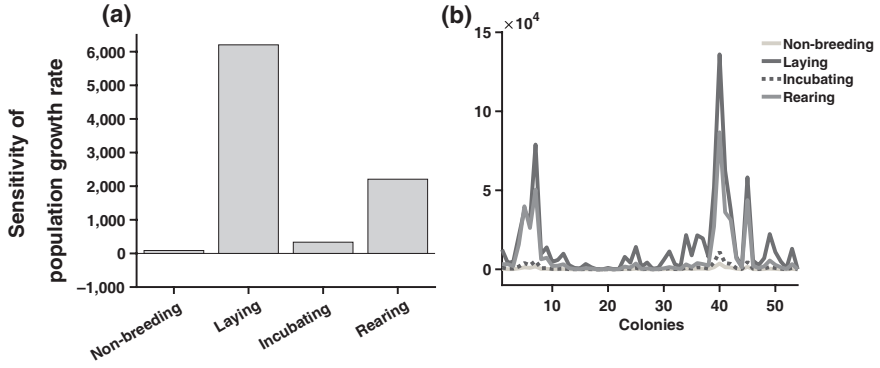

FIGURE 2 Sensitivity of the population growth rate to Antarctic sea ice conditions for the four seasons of the life cycle of emperor penguin. (a) Median of the absolute value of the sensitivity of the population growth rate calculated at each colony, at each time step, and each simulation for the RCP 8.5 scenario. (b) Median of the absolute value of the sensitivity of the population growth rate across colony. More details are shown in Figure S2

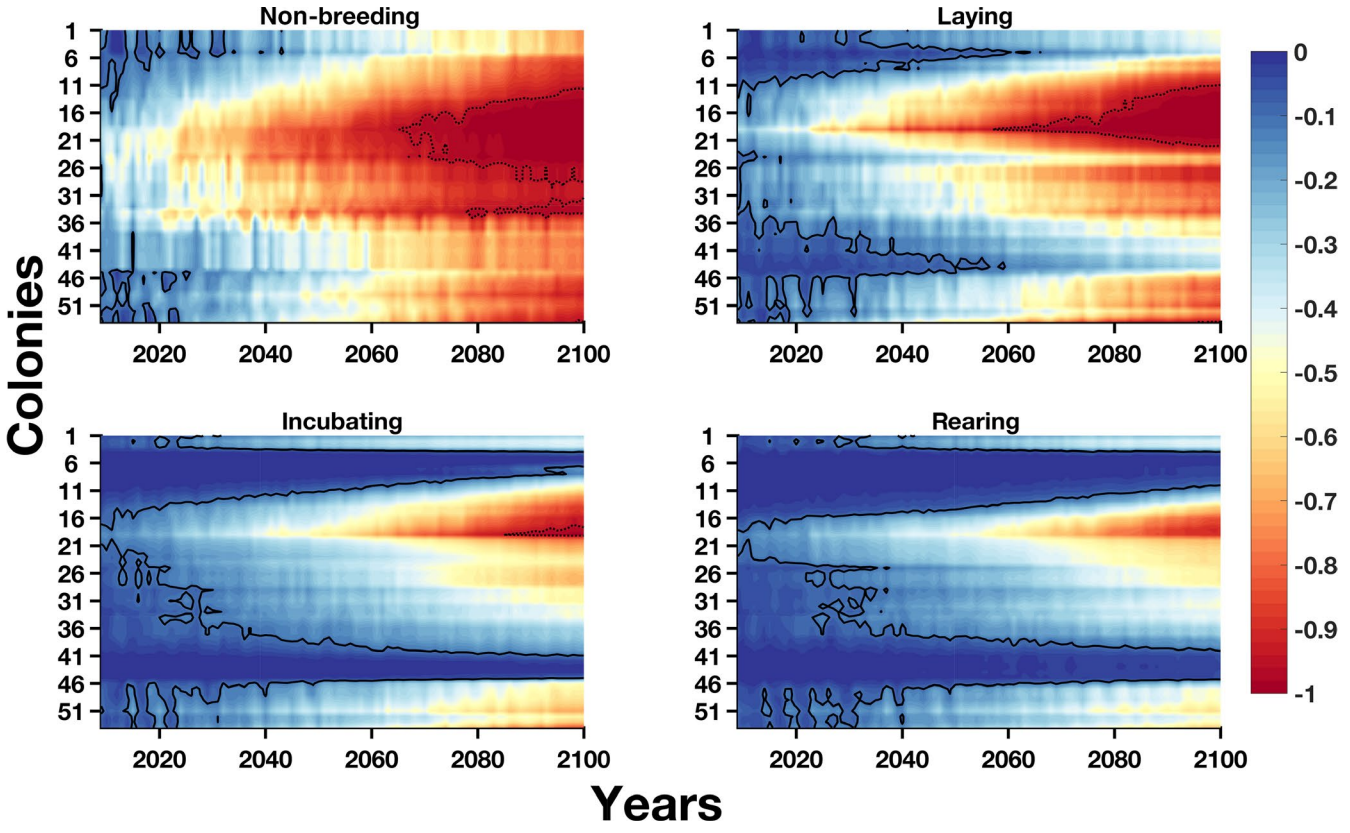

FIGURE 3 Antarctic sea ice projections using RCP 8.5. These are projections from the Community Earth System Model for each emperor penguin colony (*y*-axis) from 2009 to 2100 (*x*-axis), for each season of the emperor penguin life cycle (panels). The *y*-axis refers to the colony number used in Figure S1. Medians of the large ensemble of Antarctic sea ice concentration anomalies at each penguin colony are shown (color bar) as function of time (*x*-axis). Dotted black contour shows a 90% decline in sea ice relative to the historical mean (1979–2007), while the thick black contour shows a 10% decline

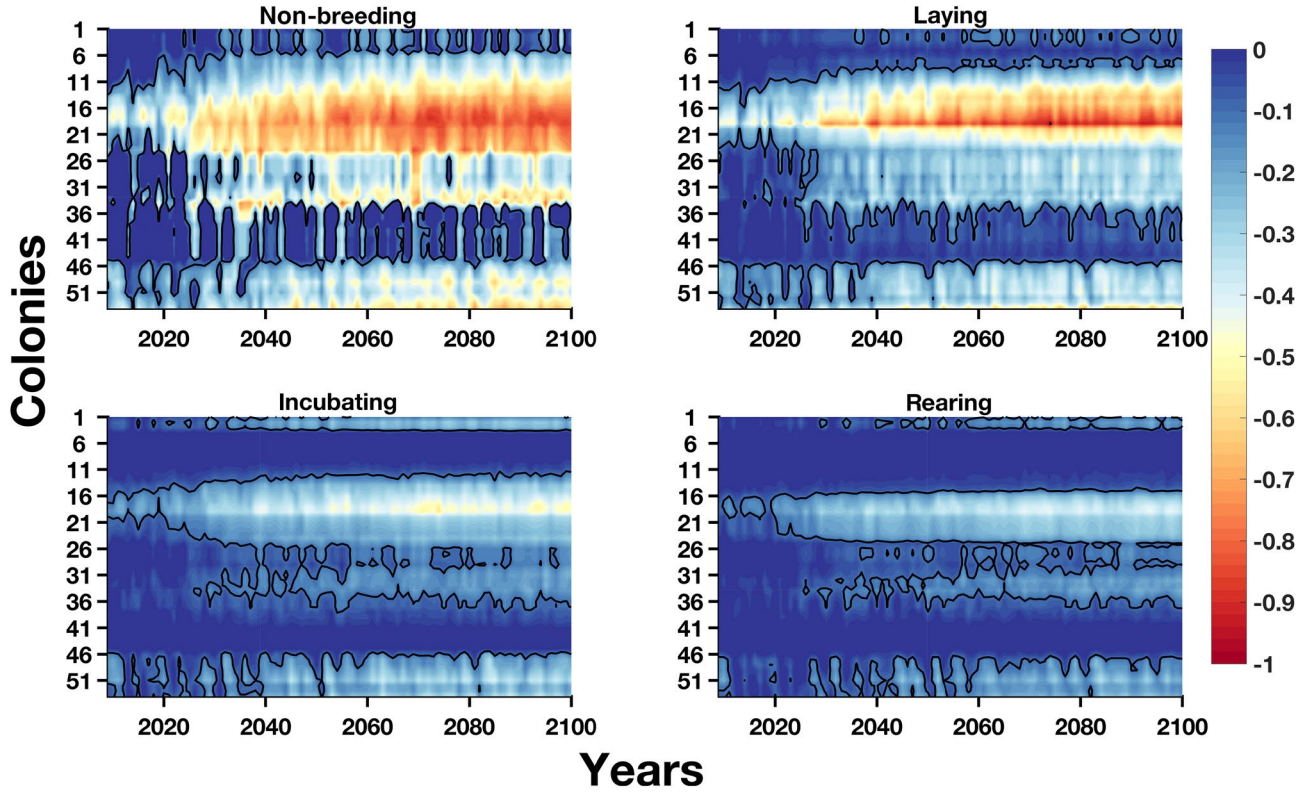

FIGURE 4 Antarctic sea ice projections using Paris Agreement's 2°C goal. Same legends as Figure 3

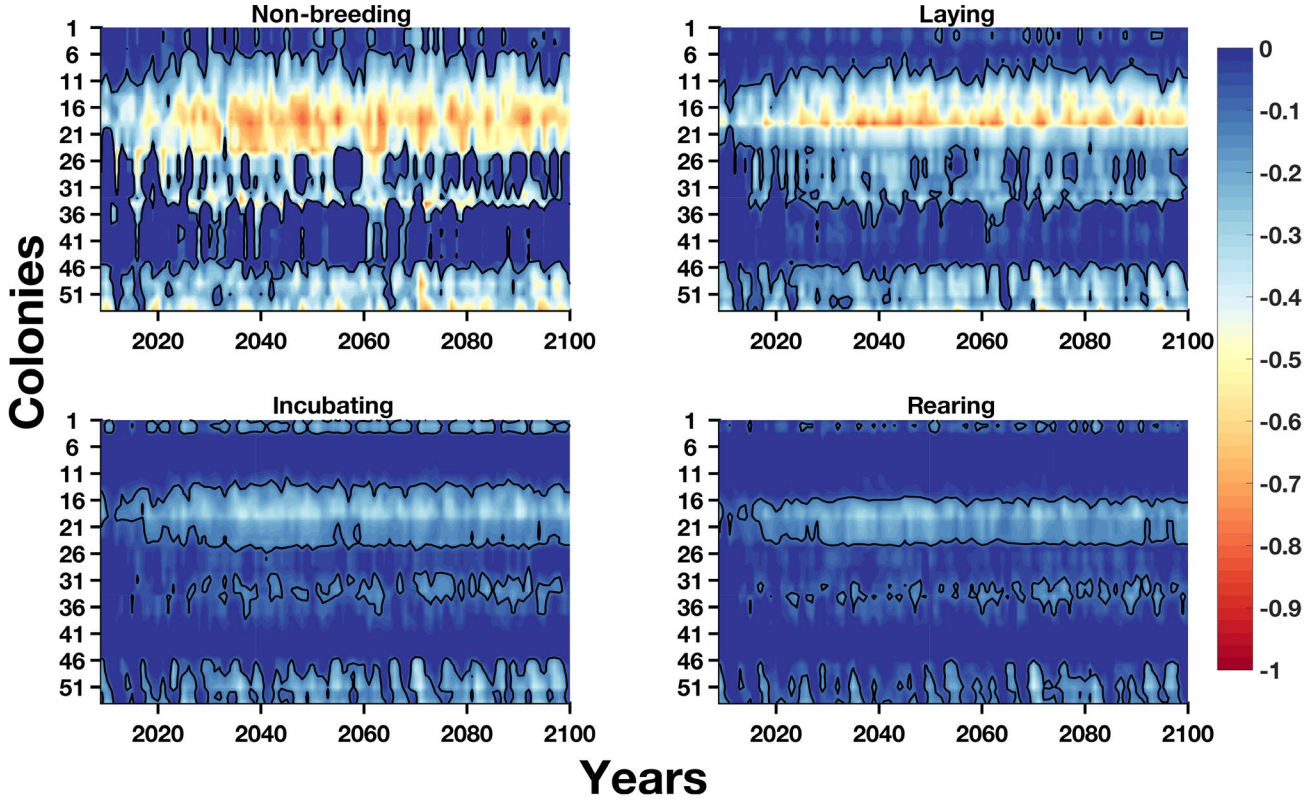

FIGURE 5 Antarctic sea ice projections using Paris Agreement's 1.5°C goal. Same legends as Figure 3

and laying seasons at the end of the century. By 2060, most colonies (except in the Eastern Weddell Sea and Ross Sea) experience declines larger than 50% relative to historical levels during the nonbreeding and laying seasons. In contrast, for the climate scenario meeting the Paris Agreement's goals, such large sea ice declines are limited to fewer colonies in Dronning, Enderby, and Kemp lands (Figure S1).

Under Paris Agreement's 1.5°C goal, most colonies experience sea ice declines smaller than 10% to their historical mean during the breeding seasons (except colonies in Dronning, Enderby, and Kemp lands).

3.3 | Emperor penguin population projections

Under the 'baseline' RCP 8.5 scenario in which greenhouse emissions remain unmitigated throughout the 21st century, by 2100 all emperor penguin colonies are projected to decline, and 43 of the 54 (80%) colonies are projected to decline by more than 90% and thus be quasiextinct (Figures 6a and 7a; Figures S3–S6). In this scenario, annual mean Antarctic sea ice extent declines by 48%, and the most endangered colonies in Queen Maud, Enderby, and Kemp Land will likely experience complete loss of sea ice during the critical laying season (Figures 2 and 3). The colonies that are projected to be quasiextinct by 2100 all experience sea ice decline larger than 50% relative to historical mean during the laying season. Globally, the total abundance of emperor penguins is projected to decline by 86% (median of projections; Figure 8) relative to its initial size if individuals do not disperse among colonies. Simultaneously, global population growth rate is projected to decrease dramatically (Figure 5; Figure S6), resulting in annual declines of 4.06% per year by the end of the century (a half-life of 17 years). Under these conditions, the species will go extinct rapidly. Furthermore, even under a dispersal scenario that leads to the most optimistic population outcome (short

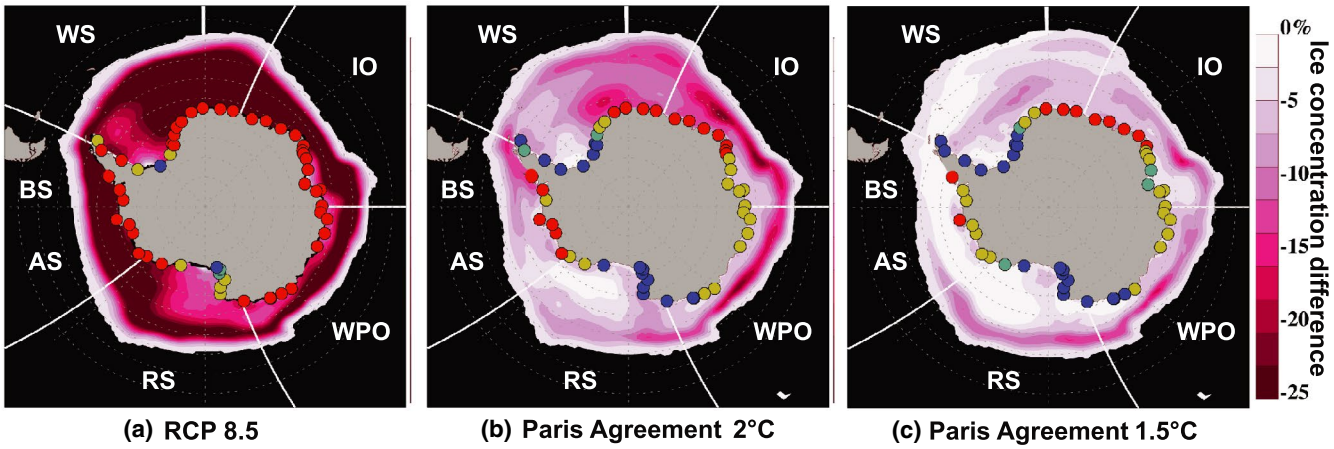

FIGURE 6 Conservation status of emperor penguin colonies by 2100 and annual mean change of sea ice concentrations (SIC) between the 20th and 21st centuries. Panels show each climate scenario without dispersal. SIC projections were obtained from the Community Earth System Model using (a) RCP 8.5, (b) Paris Agreement's 2°C goal, and (c) Paris Agreement's 1.5°C. Dots show the location of colonies (Figure S1; Table S1). Dot colors show the conservation status. Following Jenouvrier et al. (2014), 'vulnerable' (green) is a likely population decline by more than 30%; 'endangered' (yellow) is a likely population decline by more than 50%; 'quasi-extinct' (red) is a likely population decline by more than 90%. Blue color refers to populations that are not likely to decline by more than 30%. A likely outcome is defined by IPCC as a probability >66% (Tables S2–S4). AS, Amundsen Sea; BS, Bellingshausen Sea; IO, Indian Ocean; RS, Ross Sea; WPO, Western Pacific Ocean; WS, Weddell Sea

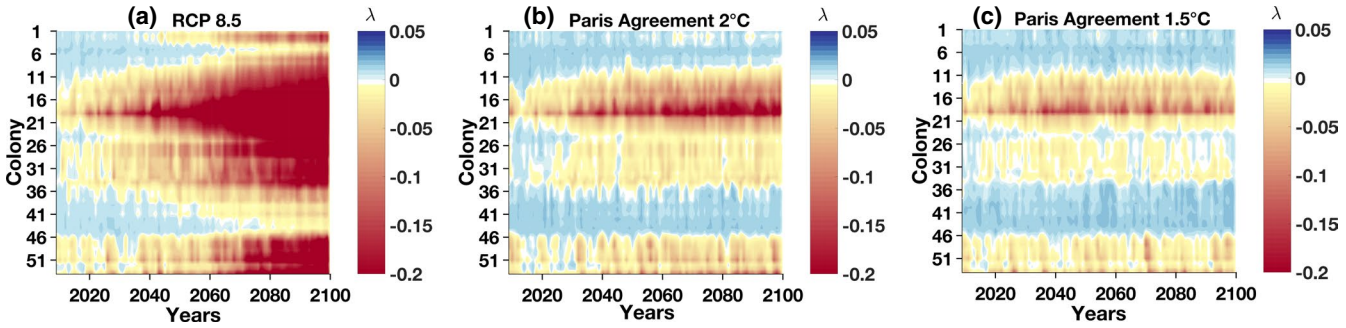

FIGURE 7 Projected intrinsic population growth rate of emperor penguin colonies through to 2100 for each climate scenario without dispersal. The figure shows the median of the year-to-year population growth rates from 2009 to 2100 for each colony. Growth rates are based on sea ice concentration anomaly projections from the Community Earth System Model using (a) RCP 8.5, (b) Paris Agreement's 2°C goal, and (c) Paris Agreement's 1.5°C. The *y*-axis refers to the colony number used in Figure S1. Blue (red) colors show a positive (negative) population growth rate. The white contour represents a null growth rate, indicating stable populations

distance of dispersal, low emigration rate, and informed search), the median of the global population is projected to decline by 81% (Figure 9a; Figure S7). Larger global declines are projected with other dispersal scenarios, up to a decline of 99% relative to its current size with long-distance dispersal and high emigration rate regardless of dispersal behavior (random or informed search). By including all uncertainties (Figure S8), the 90% confidence envelope of the global population projections by 2100 ranges from a decline of 99.2% to 67% relative to the 2009 initial size.

In contrast, under the Paris Agreement 1.5 and 2°C climate scenarios, only 10 (19%) and 17 (31%) colonies are projected to be quasiextinct by 2100, respectively (Figure 6). Under Paris 2, the annual mean sea ice extent loss by 2100 is 13%, whereas under Paris 1.5 the loss is only 5%. The colonies that are not endangered (blue colonies on Figure 6) are more likely to experience sea ice decline smaller than 10% relative to the historical mean during the four seasons of their life cycle (Figures 4 and 5). The most threatened colonies are located in eastern Antarctica where projected declines in sea ice extent are largest (Figure 6b). Colonies in the Ross Sea will experience less sea ice loss and thus are projected to increase from their current size by 2100 (Figures S2–S4). Yet, in total, 56% and 65% of emperor penguin colonies (under Paris 1.5 and 2, respectively) are likely to experience declines of 50% by 2100. As a result, the median of the global population is projected to decline by 44% under Paris 2, and by 31% under Paris 1.5 without dispersal. Despite these declines in abundance that occur in the first half of the century, population growth rates stabilize by 2100 such that the global population will be only declining at 0.07% (a half-life of 952 years) under Paris 1.5, and 0.34% (half-life of 201 years) under Paris 2. Thus, emperor penguins will persist if the Paris Agreement objectives are met, with two main refuges in the Ross and Weddell Seas. Other dispersal scenario project slightly larger global declines. For example, if individuals have high emigration rates, short-range dispersal, and select habitats nonrandomly (Figure S5), the global population will decline by 34% by 2100 under Paris 1.5. By including all uncertainties (Figure S8), the 90% confidence envelope of the global population projections by 2100 ranges from a decline of 38.6% and 49. 3% under Paris 1.5 and 2, respectively, to an increase of 161.2% and 89% under Paris 1.5 and 2, relative to the 2009 initial size.

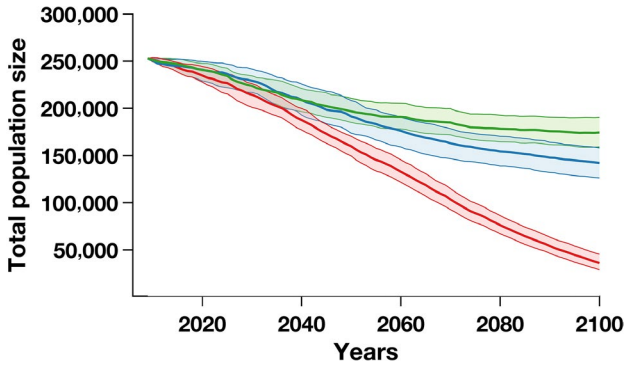

FIGURE 8 Global number of breeding pairs of emperor penguins from 2009 to 2100 projected for various climate scenarios without dispersal. This global population size is calculated using sea ice concentration anomaly projections from the Community Climate System Model using RCP 8.5 (red), Paris Agreement's 2°C goal (blue), and Paris Agreement's 1.5°C (green). The thick lines are the median and the colored areas are the 90% envelopes from stochastic simulations of population trajectories

3.4 | Uncertainties

Our projections account for uncertainty in estimates of demographic parameters and their relationship to climate, as well as temporal variance in population growth that is not related to sea ice conditions. In addition, under each climate scenario, we conduct a set of population projections using dispersal models that include no dispersal and various combinations of dispersal behaviors, including (a) high or low movement between breeding colonies; (b) two types of search strategies for new colonies (random or informed); and (c) either short- (up to 1,000 km) or long-distance movements (up to 6,000 km). In aggregate, these simulations place bounds on the degree to which emperor penguins could modulate climate effects through movement and habitat selection.

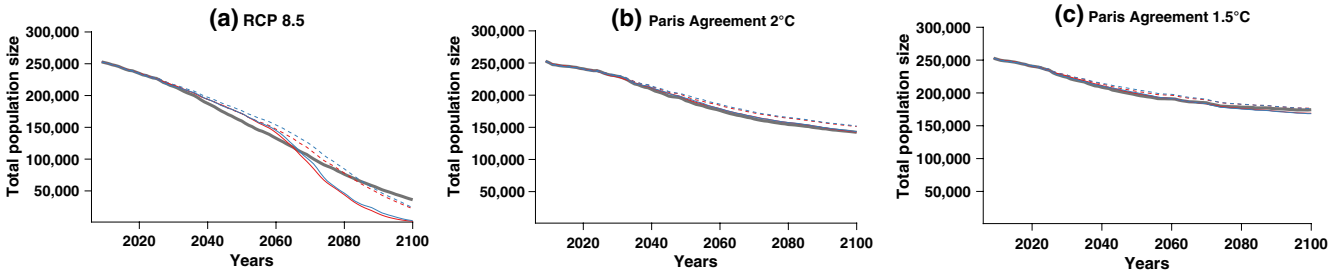

FIGURE 9 Global number of breeding pairs of emperor penguins from 2009 to 2100 projected for various dispersal and climate scenarios. These median global population sizes are calculated using sea ice concentration anomaly projections from the Community Earth System Model using (a) RCP 8.5, (b) Paris Agreement's 2°C goal, and (c) Paris Agreement's 1.5°C. Thick light gray line is the population trajectory without dispersal. Colored solid lines are population trajectories under high emigration rates, while dashed lines show low emigration rates. Blue lines are trajectories under informed search, while red lines show the random search. The distance of dispersal is large (6,000 km). Figure S7 shows the confidence envelope associated with these projections

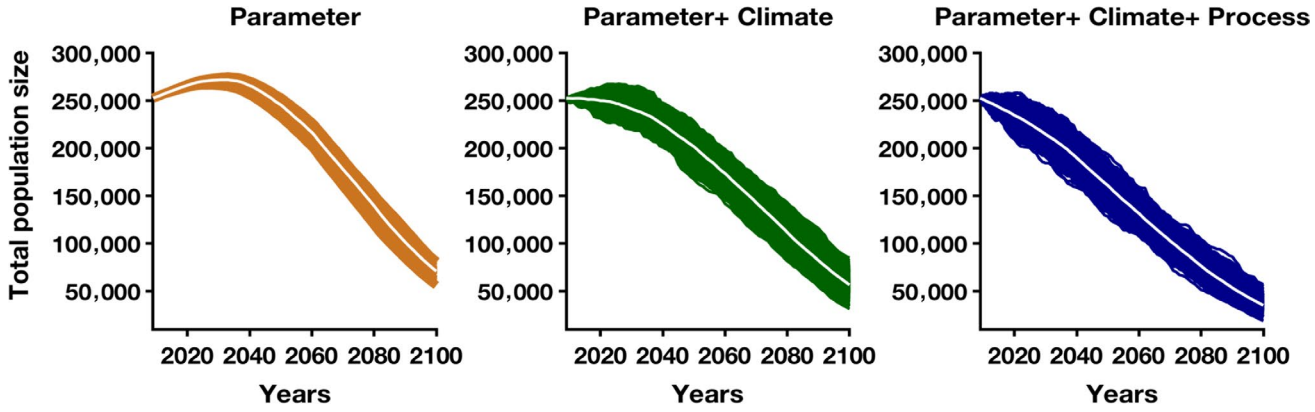

FIGURE 10 Uncertainty decomposition for the global population size of emperor penguins. The population projections at each colony are based on sea ice concentration anomaly projections from the Community Earth System Model under RCP 8.5 without dispersion. They are three main sources of uncertainty: parameter uncertainty, climate uncertainty, and process variance (colored areas). The white thick line shows the median of these projections

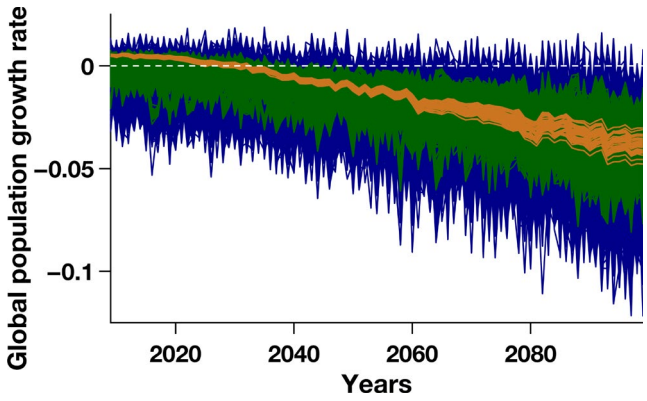

FIGURE 11 Uncertainty decomposition for annual global population growth rate of emperor penguins. Same legends as Figure 10 for colored areas. The white dashed line shows a stable population, that is, a null population growth rate

Uncertainties due to climate and environmental stochasticity are large for the population growth rate (Figure 10). Complex patterns of uncertainties occur at the level of the global population size because the model is highly nonlinear by accounting for density dependence processes and mating processes at each colony in response to sea ice (Figure 11). Structural uncertainties due to dispersal processes are relatively small (Figure 7).

Figures S3–S5 show the uncertainties of the population projections at each colony for the three climate scenarios (RCP 8.5, Paris Agreement's 2°C goal, and Paris Agreement's 1.5°C) and various dispersal scenarios contrasting short/long distance of dispersal, low/high emigration rate, and informed versus random search. Figure S7 shows the uncertainties of the global population projections according to the climate and dispersal scenarios. Figures S8–S10 summarize all the structural uncertainties in the metapopulation model for each climate scenario, and show larger confidence envelope. The violin plots illustrate the distribution of the global population sizes by 2100. For RCP 8.5 all population projections are projected to decline, while for Paris Agreement's some projections are projected to increase by 2100 but declines are still more likely. The large global population projected for some projections arises from a model without density dependence. However, expert opinion indicates 'low confidence' that populations could grow exponentially to this abundance without reaching carrying capacity; thus, this model places a maximum upper bound on potential population size.

4 | DISCUSSION

Our global demographic assessment of the potential impacts of meeting the Paris Agreement for an iconic species threatened by future climate change, shows that global climate policy has the capacity to halt future projected declines of emperor penguins in ways that their intrinsic biological properties (i.e., dispersal abilities) do not. For the first time we take advantage of newly developed mitigation ensembles of fully coupled climate simulations consistent with meeting the Paris Agreement objectives to derive robust projections of future population dynamics and species persistence. Using these ensembles of internally consistent coupled climate simulations permits us to project temporal and spatial emperor penguin population dynamics from 2010 to 2100, and track the continually changing trajectories of interconnected populations across the species' polar range.

The Paris Agreement climate targets lead to dramatically larger populations of emperor penguins than baseline climate scenarios, irrespective of dispersal or density dependence. Our projections account for uncertainty in estimates of demographic parameters and their relationship to climate, as well as temporal variance in population growth that is not related to sea ice conditions. Under each climate scenario, the CESM ensemble also allows us to explicitly include uncertainty in future climate due to internal climate variability. Additionally, comparison among projections that included different assumptions regarding penguin dispersal and carrying capacity indicated that our qualitative conclusions were extremely robust to this conclusion (Figures S5–S8).

4.1 | Climate and demographic uncertainties

Uncertainty is central to population forecasting and enters in every step, from climate modeling (e.g., uncertainty in current climate conditions and future climate change) to demographic modeling (e.g., uncertainty in the responses of vital rates to climate parameters, residual vital rate covariation, etc.) to population modeling (e.g., uncertainty in population abundance and stage structure; Iles & Jenouvrier, 2019). Forecasts that fail to include these key sources of uncertainty will be falsely overconfident, eroding trust in ecological science and hindering ecological understanding (Clark et al., 2001; Dietze, 2017). Forecasting therefore requires a quantification of uncertainty in each model component, and importantly, full propagation of these uncertainties to forecasts.

Forecast uncertainty is dominated by different processes across various spatial and temporal horizons (Dietze, 2017; Hawkins & Sutton, 2009). Here we found that the uncertainties related to climate internal variability and unexplained temporal variance in vital rates (process variance) are relatively large (Figure 10). If these uncertainties are ignored, the global number of breeding pairs is projected to increase from 2009 to ~2033, while no such increase is projected when all uncertainties were accounted for (Figure 10). In addition, if these uncertainties are ignored, the global population size by 2100 is twice as large than that when all uncertainties are accounted for (medians: 71,080 vs. 35,150). Indeed, an increase in sea ice variability is likely to reduce the stochastic population growth rate of emperor penguin, at least when the average sea ice conditions are not far from historical sea ice mean (see figure 6a in Jenouvrier et al., 2012). In addition, an increase in unexplained temporal variance in vital rate is likely to reduce the stochastic population growth rate (Koons, Pavard, Baudisch, & Metcalf, 2009; Tuljapurkar & Orzack, 1980). Hence, including both climate internal variability and process variance reduce the projected number of breeding pairs, and affect strongly the projected trajectory throughout the century (see also figure 4c in Jenouvrier, 2013). These results emphasize the importance for incorporating the natural climate variability and non-stationary climate dynamics predicted by an ensemble of climate models (Jenouvrier 2013).

There are three sources of uncertainty in climate model projections (Hawkins & Sutton, 2009) which include (a) scenario uncertainty associated with the future greenhouse gas emissions; (b) internal variability associated with the chaotic nature of the climate system; and (c) model structural uncertainty due to errors in the models themselves. In this study, we assess the role of the greenhouse gas scenario in driving differences in projected emperor penguin responses to climate change, hence account for scenario uncertainty. In doing so, we consider model simulations with the RCP 8.5 emissions scenario (Van Vuuren et al., 2011) which has increasing greenhouse gas emissions over the 21st century and reaches a global radiative forcing of 8.5 W/m^2 and compare these to model simulations which use unique Paris target forcing scenarios (Sanderson et al., 2017). These Paris target scenarios were explicitly designed to reach 1.5 or 2°C of global average warming by 2100 as outlined in the Paris Agreement. In addition, we account for the uncertainty due to internal variability using a large ensemble of simulations with the CESM1 (Hurrell et al., 2013; Kay et al., 2015). The ensemble simulation sets use the same model and forcing but differ very slightly in their initial state. This results in a different time evolution of climate conditions due to chaotic dynamics and allows us to isolate the uncertainty in sea ice projections that is associated with internal variability. Finally, here we do not consider the uncertainty associated with model structure. This model structural uncertainty can be large for projections of Antarctic sea ice (e.g., IPCC AR5, Chapter 12; Turner, Bracegirdle, Phillips, Marshall, & Hosking, 2013), with important consequences for emperor penguin population projections (Jenouvrier et al., 2012). However, the Paris target forcing scenario has only been applied in a single model (the CESM1) and so it is not possible to assess model structural uncertainty with this scenario. Additionally, most of the available climate model projections do not include a large ensemble of members and thus we are not able to assess the role of internal variability in projection uncertainty for those models. Given this, and the very good quality of the CESM1 Antarctic sea ice simulation for present day conditions (Figure 1), our use of the CESM1 simulations to characterize evolving sea ice conditions under the different scenarios provides a reasonable approach to diagnose the role of meeting the Paris Agreement targets for emperor penguins. In addition, the largest differences between CESM1 sea ice simulations and observations over the historical period, occur during seasons or regions for which sea ice conditions have little effect on the emperor penguin population growth rates (Figure 2), hence our results are robust to these climate biases. Finally, while they are large uncertainties in projected sea ice loss in Antarctica (Collins et al., 2013), we have a high confidence on the avoided impacts for emperor penguins in 1.5 or 2°C climate futures relative to a 'business-as-usual' scenario.

4.2 | Emperor penguin responses to climate change

Adaptive capacity and dispersal ability are two key attributes that affect the resilience of species to climate change (Williams, Shoo, Isaac, Hoffmann, & Langham, 2008). In our study, incorporating dispersal led to steeper population declines by 2100 than models in which individuals were completely site-faithful under RCP 8.5 (Figure 7). This counterintuitive result occurs because dispersal allows poor quality habitats that would otherwise be sequestered to function as connected demographic sinks that rapidly deplete the entire metapopulation (Jenouvrier et al., 2017). The adaptive capacity of emperor penguins is unknown, but is likely limited because they have a long life spans, delayed maturity, and low reproductive rates, coupled with low genetic diversity (Younger et al., 2017). The biological capacity for emperor penguins to 'cope' with climate change through adaptation or dispersal to suitable habitats is therefore likely to be minimal (but see Younger et al., 2015). Nevertheless, here we have demonstrated that global climate policy has the capacity to safeguard the future of emperor penguins in ways that their

intrinsic biological properties do not as Paris Agreement climate scenarios resulted in dramatically higher population viability than a baseline scenario.

4.3 | Climate change mitigation

Globally, the projected abundance of emperor penguins in 2100 was higher under Paris 1.5 than Paris 2. Additionally, the temporal dynamics and end-of-century abundance of individual colonies often differed markedly under these two climate thresholds. For example, the well-studied breeding colony at Pointe Géologie experiences continued declines throughout the 21st century under 2°C warming, but remains largely stable, especially in the second half of the century under 1.5°C (Figures S3–S5). Additionally, the Cape Darnley breeding colony declines precipitously under Paris 2 and is rapidly trending toward extinction at 2100, but has largely stabilized by 2100 (albeit at a lower abundance) under Paris 1.5. This 'half degree difference' has also recently been shown to affect projected range sizes for a large proportion of insects, vertebrates, and plants (Warren, Price, Graham, et al., 2018). While this half-degree difference is likely to affect many climate properties, in polar systems it will have especially large impacts on sea ice conditions. For example, the chance that the Arctic experiences an ice-free year by 2100 is 30% under 1.5° of warming, but rises to 100% under 2° of warming (Jahn, 2018). Here we showed that in Antarctica (Figures 4 and 5), the projected response of sea ice to this half-degree difference varies across regions, resulting in extremely strong effects on particular emperor penguin colonies (Figures S3–S5).

Emperor penguins are considered 'indicators' of climate change in the Southern Ocean because they are highly sensitive to environmental conditions in multiple stages of their annual cycle and across large spatial extents (Barbraud & Weimerskirch, 2001). Yet, many other polar species across a diversity of life histories are also tied to sea ice conditions (Thomas & Dieckmann, 2008). Ice-dependent species occupy all levels of the food web in Antarctica, including primary producers (e.g., ice algae and phytoplankton), zooplankton (e.g., krill), and secondary and tertiary consumers (e.g., Antarctic silverfish, Weddell seals: *Leptonychotes weddellii*, Snow petrels: *Pagodroma nivea*). Similarly strong linkages to sea ice exist for species in the Arctic (e.g., for Polar bears: *Ursus maritimus*; Hunter et al., 2010) where climate change is progressing even more rapidly. It is therefore likely that meeting the Paris Agreement objectives, or failing to do so, will have wide-ranging consequences that extend far beyond the effects we demonstrated for emperor penguins.

Climate change may combine with and potentially exacerbate other pressures that influence the viability of polar species (Rintoul et al., 2018). For example, melting sea ice may increase human access to new fishing areas, increasing competition with Antarctic predators such as emperor penguins. Similarly, range shifts of other species will likely alter the composition of marine communities, with potentially important impacts across the food web. These interactive and multispecies effects are difficult to anticipate, and represent an important avenue of future research. Nevertheless, our study emphasizes that near-term global policy decisions over the next decade will have dramatic impacts on the viability of an iconic Antarctic predator, and will likely shape the future of earth's biota more generally.

ACKNOWLEDGEMENTS

We acknowledge Institute Paul Emile Victor (Programme IPEV 109), and by Terres Australes et Antarctiques Françaises for TA penguin data. We acknowledge D. Besson and K. Delord for TA penguin data management. We acknowledge the support of NSF OPP 1643901 (PICA) to SJ and RJ, and NSF OPP 1744794 to SJ, SL and ML.

CONFLICT OF INTEREST

The authors declare no competing interests.

AUTHOR CONTRIBUTIONS

S.J. and M.H. conceptualized project idea; C.B. and H.W. curated emperor penguin data; M.H. and L.L. managed climate data; S.J., M.H., J.G., and H.C. developed the climate-dependent-metapopulation model; S.J., M.H. and L.L. performed climate experiments and population projections; S.J. and D.I. analyzed and synthesized uncertainties data; S.J., L.L., M.H., S.L., and D.I. performed data visualization and prepared figures; S.J., M.L., R.J., and M.H. acquired funds; S.J., D.I. and M.H. wrote the manuscript; all authors discussed the interpretation of data and edited the manuscript.

DATA AVAILABILITY STATEMENT

All data are available in the main text or the Supporting Information. Detailed code and materials used in the analysis will be available on HAL repository (https://hal.archives-ouvertes.fr) following publication.

ORCID

Stéphanie Jenouvrier https://orcid.org/0000-0003-3324-2383

David Iles https://orcid.org/0000-0002-7251-4938

REFERENCES

Abadi, F., Barbraud, C., & Gimenez, O. (2017). Integrated population modeling reveals the impact of climate on the survival of juvenile emperor penguins. *Global Change Biology*, *23*, 1353–1359. https://doi.org/10.1111/gcb.13538

Ainley, D., Ballard, G., Blight, L. K., Ackley, S., Emslie, S. D., Lescroël, A., … Woehler, E. (2010). Impacts of cetaceans on the structure of southern ocean food webs. *Marine Mammal Science*, *26*, 482–498. https://doi.org/10.1111/j.1748-7692.2009.00337.x

Barbraud, C., & Weimerskirch, H. (2001). Emperor penguins and climate change. *Nature*, *411*, 183–186. https://doi.org/10.1038/35075554

Bowler, D. E., & Benton, T. G. (2005). Causes and consequences of animal dispersal strategies: Relating individual behaviour to spatial dynamics. *Biological Reviews*, *80*, 205–225. https://doi.org/10.1017/S1464793104006645

Clark, J. S., Carpenter, S. R., Barber, M., Collins, S., Dobson, A., Foley, J. A., … Pringle, C. (2001). Ecological forecasts: An emerging imperative. *Science*, *293*, 657–660. https://doi.org/10.1126/science.293.5530.657

Clucas, G. V., Younger, J. L., Kao, D., Emmerson, L., Southwell, C., Wienecke, B., … Hart, T. (2018). Comparative population genomics reveals key barriers to dispersal in southern ocean penguins. *Molecular Ecology*, *27*, 4680–4697. https://doi.org/10.1111/mec.14896

Collins, M., Knutti, R., Arblaster, J., Dufresne, J. L., Fichefet, T., Friedlingstein, P., … Shongwe, M. (2013). Long-term climate change: Projections, commitments and irreversibility. In T. F. Stocker, D. Qin, G.-K. Plattner, M. M. B. Tignor, S. K. Allen, J. Boschung, Y. Alexander Nauels, V. B. Xia, & P. M. Midgley (Eds.), *Climate change 2013 – The physical science basis: Contribution of working group I to the fifth assessment report of the Intergovernmental Panel on Climate Change* (pp. 1029–1136). New York, NY: Cambridge University Press.

Dietze, M. C. (2017). *Ecological forecasting*. Princeton, NJ: Princeton University Press.

Doligez, B., Danchin, E., & Clobert, J. (2002). Public information and breeding habitat selection in a wild bird population. *Science*, *297*, 1168–1170. https://doi.org/10.1126/science.1072838

Ehrlén, J., & Morris, W. F. (2015). Predicting changes in the distribution and abundance of species under environmental change. *Ecology Letters*, *18*, 303–314. https://doi.org/10.1111/ele.12410

Foden, W. B., Butchart, S. H., Stuart, S. N., Vié, J. C., Akçakaya, H. R., Angulo, A., … Donner, S. D. (2013). Identifying the world's most climate change vulnerable species: A systematic trait-based assessment of all birds, amphibians and corals. *PLoS ONE*, *8*, e65427. https://doi.org/10.1371/journal.pone.0065427

Forcada, J., & Trathan, P. N. (2009). Penguin responses to climate change in the southern ocean. *Global Change Biology*, *15*, 1618–1630. https://doi.org/10.1111/j.1365-2486.2009.01909.x

Fretwell, P. T., LaRue, M. A., Morin, P., Kooyman, G. L., Wienecke, B., Ratcliffe, N., … Trathan, P. N. (2012). An emperor penguin population estimate: The first global, synoptic survey of a species from space. *PLoS ONE*, *7*, e33751. https://doi.org/10.1371/journal.pone.0033751

Fretwell, P. T., & Trathan, P. N. (2009). Penguins from space: Faecal stains reveal the location of emperor penguin colonies. *Global Ecology and Biogeography*, *18*, 543–552. https://doi.org/10.1111/j.1466-8238.2009.00467.x

Fretwell, P. T., Trathan, P. N., Wienecke, B., & Kooyman, G. L. (2014). Emperor penguins breeding on iceshelves. *PLoS ONE*, *9*, e85285. https://doi.org/10.1371/journal.pone.0085285

Gauthier, G., Péron, G., Lebreton, J.-D., Grenier, P., & van Oudenhove, L. (2016). Partitioning prediction uncertainty in climate-dependent population models. *Proceedings of the Royal Society B: Biological Sciences*, *283*(1845), 20162353. https://doi.org/10.1098/rspb.2016.2353

Hawkins, E., & Sutton, R. (2009). The potential to narrow uncertainty in regional climate predictions. *Bulletin of the American Meteorological Society*, *90*, 1095–1108. https://doi.org/10.1175/2009BAMS2607.1

Hunter, C., Caswell, H., Runge, M., Regehr, E., Amstrup, S., & Stirling, I. (2010). Climate change threatens polar bear populations: A stochastic demographic analysis. *Ecology*, *91*, 2883–2897. https://doi.org/10.1890/09-1641.1

Hurrell, J. W., Holland, M. M., Gent, P. R., Ghan, S., Kay, J. E., Kushner, P. J., … Marshall, S. (2013). The community earth system model: A framework for collaborative research. *Bulletin of the American Meteorological Society*, *94*, 1339–1360. https://doi.org/10.1175/BAMS-D-12-00121.1

Iles, D., & Jenouvrier, S. (2019). *Effects of climate change on birds*, *chap. 12: Projected population consequences of climate change* (pp. 147–164). Oxford, UK: Oxford Univsersity Press.

Iles, D. T., Williams, N. M., & Crone, E. E. (2018). Source-sink dynamics of bumblebees in rapidly changing landscapes. *Journal of Applied Ecology*, *55*, 2802–2811. https://doi.org/10.1111/1365-2664.13175

Jahn, A. (2018). Reduced probability of ice-free summers for 1.5°C compared to 2°C warming. *Nature Climate Change*, *8*, 409–413. https://doi.org/10.1038/s41558-018-0127-8

Jenouvrier, S. (2013). Impacts of climate change on avian populations. *Global Change Biology*, *19*, 2036–2057. https://doi.org/10.1111/gcb.12195

Jenouvrier, S., Barbraud, C., Weimerskirch, H., & Caswell, H. (2009). Limitation of population recovery: A stochastic approach to the case of the emperor penguin. *Oikos*, *118*, 1292–1298. https://doi.org/10.1111/j.1600-0706.2009.17498.x

Jenouvrier, S., Caswell, H., Barbraud, C., Holland, M., Stroeve, J., & Weimerskirch, H. (2009). Demographic models and IPCC climate projections predict the decline of an emperor penguin population. *Proceedings of the National Academy of Sciences of the United States of America*, *106*, 1844–1847. https://doi.org/10.1073/pnas.0806638106

Jenouvrier, S., Caswell, H., Barbraud, C., & Weimerskirch, H. (2010). Mating behavior, population growth, and the operational sex ratio: A periodic two-sex model approach. *The American Naturalist*, *175*, 739–752. https://doi.org/10.1086/652436

Jenouvrier, S., Garnier, J., Patout, F., & Desvillettes, L. (2017). Influence of dispersal processes on the global dynamics of Emperor penguin, a species threatened by climate change. *Biological Conservation*, *212*, 63–73. https://doi.org/10.1016/j.biocon.2017.05.017

Jenouvrier, S., Holland, M., Stroeve, J., Barbraud, C., Weimerskirch, H., Serreze, M., & Caswell, H. (2012). Effects of climate change on an emperor penguin population: Analysis of coupled demographic and climate models. *Global Change Biology*, *18*, 2756–2770. https://doi.org/10.1111/j.1365-2486.2012.02744.x

Jenouvrier, S., Holland, M., Stroeve, J., Serreze, M., Barbraud, C., Weimerskirch, H., & Caswell, H. (2014). Projected continent-wide declines of the emperor penguin under climate change. *Nature Climate Change*, *4*, 715–718. https://doi.org/10.1038/nclimate2280

Kay, J. E., Deser, C., Phillips, A., Mai, A., Hannay, C., Strand, G., … Vertenstein, M. (2015). The community earth system model (CESM) large ensemble project: A community resource for studying climate change in the presence of internal climate variability. *Bulletin of the American Meteorological Society*, *96*, 1333–1349. https://doi.org/10.1175/BAMS-D-13-00255.1

Knutti, R., & Sedláček, J. (2013). Robustness and uncertainties in the new CMIP5 climate model projections. *Nature Climate Change*, *3*, 369–373. https://doi.org/10.1038/nclimate1716

Koons, D. N., Pavard, S., Baudisch, A., & Metcalf, C. J. E. (2009). Is life-history buffering or lability adaptive in stochastic environments? *Oikos*, *118*, 972–980. https://doi.org/10.1111/j.1600-0706.2009.16399.x

Kristan, W. B. III. (2003). The role of habitat selection behavior in population dynamics: Source–sink systems and ecological traps. *Oikos*, *103*, 457–468. https://doi.org/10.1034/j.1600-0706.2003.12192.x

La Mesa, M., Catalano, B., Russo, A., Greco, S., Vacchi, M., & Azzali, M. (2010). Influence of environmental conditions on spatial distribution and abundance of early life stages of Antarctic silverfish, *Pleuragramma antarcticum* (Nototheniidae), in the Ross Sea. *Antarctic Science*, *22*, 243–254. https://doi.org/10.1017/s0954102009990721

Lande, R. (1993). Risks of population extinction from demographic and environmental stochasticity and random catastrophes. *The American Naturalist*, *142*, 911–927. https://doi.org/10.1086/285580

Lande, R., Engen, S., & Sæther, B.-E. (1999). Spatial scale of population synchrony: Environmental correlation versus dispersal and density regulation. *The American Naturalist*, *154*, 271–281. https://doi.org/10.1086/303240

Landrum, L. L., Holland, M. M., Raphael, M. N., & Polvani, L. M. (2017). Stratospheric ozone depletion: An unlikely driver of the regional trends in Antarctic sea ice in austral fall in the late twentieth century.

Geophysical Research Letters, *44*(21), 11062–11070. https://doi.org/10.1002/2017GL075618

LaRue, M. A., Kooyman, G., Lynch, H. J., & Fretwell, P. (2015). Emigration in emperor penguins: Implications for interpretation of long-term studies. *Ecography*, *38*, 114–120. https://doi.org/10.1111/ecog.00990

Massom, R., Hill, K., Barbraud, C., Adams, N., Ancel, A., Emmerson, L., & Pook, M. (2009). Fast ice distribution in Adélie Land, East Antarctica: Interannual variability and implications for emperor penguins *Aptenodytes forsteri*. *Marine Ecology Progress Series*, *374*, 243–257. https://doi.org/10.3354/meps07734

McRae, B. H., Schumaker, N. H., McKane, R. B., Busing, R. T., Solomon, A. M., & Burdick, C. A. (2008). A multi-model framework for simulating wildlife population response to land-use and climate change. *Ecological Modelling*, *219*, 77–91. https://doi.org/10.1016/j.ecolmodel.2008.08.001

Meinshausen, M., Smith, S. J., Calvin, K., Daniel, J. S., Kainuma, M. L. T., Lamarque, J.-F., … van Vuuren, D. P. (2011). The RCP greenhouse gas concentrations and their extensions from 1765 to 2300. *Climatic Change*, *109*, 213–241. https://doi.org/10.1007/s10584-011-0156-z

Meyer, B., Freier, U., Grimm, V., Groeneveld, J., Hunt, B. P. V., Kerwath, S., … Yilmaz, N. I. (2017). The winter pack-ice zone provides a sheltered but food-poor habitat for larval Antarctic krill. *Nature Ecology & Evolution*, *1*, 1853–1861. https://doi.org/10.1038/s41559-017-0368-3

Nakicenovic, N., Alcamo, J., Grubler, A., Riahi, K., Roehrl, R., Rogner, H. H., & Victor, N. (2000). *Special report on emissions scenarios (SRES), a special report of working group III of the Intergovernmental Panel on Climate Change*. Cambridge, UK: Cambridge University Press.

Prevost, J. (1961). *Expéditions polaires françaises*, *vol. 222*, *chap. Ecologie du manchot empereur* (pp. 1–204). Paris, France: Hermann Press.

Rintoul, S. R., Chown, S. L., DeConto, R. M., England, M. H., Fricker, H. A., Masson-Delmotte, V., … Xavier, J. C. (2018). Choosing the future of Antarctica. *Nature*, *558*, 233–241. https://doi.org/10.1038/s41586-018-0173-4

Rogelj, J., Popp, A., Calvin, K. V., Luderer, G., Emmerling, J., Gernaat, D., … Krey, V. (2018). Scenarios towards limiting global mean temperature increase below 1.5°C. *Nature Climate Change*, *8*, 325–332. https://doi.org/10.1038/s41558-018-0091-3

Ropert-Coudert, Y., Chiaradia, A., Ainley, D., Barbosa, A., Boersma, P. D., Brasso, R., … Trathan, P. N. (2019). Happy feet in a hostile world? The future of penguins depends on proactive management of current and expected threats. *Frontiers in Marine Science*, *6*, 248. https://doi.org/10.3389/fmars.2019.00248

Sanderson, B. M., & Knutti, R. (2016). Delays in US mitigation could rule out Paris targets. *Nature Climate Change*, *7*, 92–94. https://doi.org/10.1038/nclimate3193

Sanderson, B. M., Xu, Y., Tebaldi, C., Wehner, M., O'Neill, B. C., Jahn, A., … Knutti, R. (2017). Community climate simulations to assess avoided impacts in 1.5 and 2°C futures. *Earth System Dynamics*, *8*, 827–847. https://doi.org/10.5194/esd-8-827-2017

Schurr, F. M., Pagel, J., Cabral, J. S., Groeneveld, J., Bykova, O., O'Hara, R. B., … Zimmermann, N. E. (2012). How to understand species' niches and range dynamics: A demographic research agenda for biogeography. *Journal of Biogeography*, *39*, 2146–2162. https://doi.org/10.1111/j.1365-2699.2012.02737.x

Stocker, T., Qin, D., Plattner, G. K., Tignor, M., Allen, S. K., Boschung, J., … Midgley, P. M. (2013) *IPCC 2013: The physical science basis. Contribution of working group I to the fifth assessment report of the Intergovernmental Panel on Climate Change*. Cambridge, UK and New York, NY: Cambridge University Press.

Thomas, D. N., & Dieckmann, G. S. (2008). *Sea ice: An introduction to its physics, chemistry, biology and geology*. New York, NY: John Wiley & Sons.

Travis, J. M. J., Delgado, M., Bocedi, G., Baguette, M., Bartoń, K., Bonte, D., … Bullock, J. M. (2013). Dispersal and species responses to climate change. *Oikos*, *122*, 1532–1540. https://doi.org/10.1111/j.1600-0706.2013.00399.x

Travis, J. M. J., Mustin, K., Bartoń, K. A., Benton, T. G., Clobert, J., Delgado, M. M., … Bonte, D. (2012). Modelling dispersal: An eco-evolutionary framework incorporating emigration, movement, settlement behaviour and the multiple costs involved. *Methods in Ecology and Evolution*, *3*, 628–641. https://doi.org/10.1111/j.2041-210X.2012.00193.x

Tuljapurkar, S., & Orzack, S. (1980). Population dynamics in variable environments I. Long-run growth rates and extinction. *Theoretical Population Biology*, *18*, 314–342. https://doi.org/10.1016/0040-5809(80)90057-X

Turner, J., Bracegirdle, T. J., Phillips, T., Marshall, G. J., & Hosking, J. S. (2013). An initial assessment of Antarctic Sea ice extent in the CMIP5 models. *Journal of Climate*, *26*, 1473–1484. https://doi.org/10.1175/JCLI-D-12-00068.1

United Nations Framework Convention on Climate Change (UNFCCC). (2015). The Paris Agreement. Technical Report United Nations Framework Convention on Climate Change.

Van Vuuren, D. P., Edmonds, J., Kainuma, M., Riahi, K., Thomson, A., Hibbard, K., … Rose, S. K. (2011). The representative concentration pathways: An overview. *Climatic Change*, *109*, 5–31. https://doi.org/10.1007/s10584-011-0148-z

Warren, R., Price, J., Graham, E., Forstenhaeusler, N., & VanDerWal, J. (2018). The projected effect on insects, vertebrates, and plants of limiting global warming to 1.5°C rather than 2°C. *Science*, *360*(6390), 791–795. https://doi.org/10.1126/science.aar3646

Warren, R., Price, J., VanDerWal, J., Cornelius, S., & Sohl, H. (2018). The implications of the United Nations Paris Agreement on climate change for globally significant biodiversity areas. *Climatic Change*, *147*, 395–409. https://doi.org/10.1007/s10584-018-2158-6

Wienecke, B. (2011). Review of historical population information of emperor penguins. *Polar Biology*, *34*, 153–167. https://doi.org/10.1007/s00300-010-0882-0

Williams, S. E., Shoo, L. P., Isaac, J. L., Hoffmann, A. A., & Langham, G. (2008). Towards an integrated framework for assessing the vulnerability of species to climate change. *PLOS Biology*, *6*, e325. https://doi.org/10.1371/journal.pbio.0060325

Younger, J. L., Clucas, G. V., Kao, D., Rogers, A. D., Gharbi, K., Hart, T., & Miller, K. J. (2017). The challenges of detecting subtle population structure and its importance for the conservation of emperor penguins. *Molecular Ecology*, *26*, 3883–3897. https://doi.org/10.1111/mec.14172

Younger, J. L., Clucas, G. V., Kooyman, G., Wienecke, B., Rogers, A. D., Trathan, P. N., … Miller, K. J. (2015). Too much of a good thing: Sea ice extent may have forced emperor penguins into refugia during the last glacial maximum. *Global Change Biology*, *21*, 2215–2226. https://doi.org/10.1111/gcb.12882

Zimmer, I., Wilson, R., Gilbert, C., Beaulieu, M., Ancel, A., & Plötz, J. (2008). Foraging movements of emperor penguins at Pointe Géologie, Antarctica. *Polar Biology*, *31*, 229–243. https://doi.org/10.1007/s00300-007-0352-5

SUPPORTING INFORMATION

Additional supporting information may be found online in the Supporting Information section.

How to cite this article: Jenouvrier S, Holland M, Iles D, et al. The Paris Agreement objectives will likely halt future declines of emperor penguins. *Glob Change Biol*. 2019;00:1–15. https://doi.org/10.1111/gcb.14864